Reversing the Native Aerobic Oxidation Reactivity of Graphitic Carbon: Heterogeneous Metal-Free Alkene Hydrogenation

Reversing The Native Aerobic Oxidation Reactivity Of Graphitic Carbon: Heterogeneous Metal-Free Alkene Hydrogenation

Alexander T. Murray and Yogesh Surendranath*

Department of Chemistry, Massachusetts Institute of Technology, Cambridge, Massachusetts 02139, United States.

KEYWORDS Hydrogenation, Carbon Black, Carbocatalysis, Diimide, Alkene

ABSTRACT: Commercially available carbon blacks serve as effective metal-free catalysts for the selective hydrogenation of carbon-carbon multiple bonds under aerobic conditions using hydrazine as the terminal reductant. The reaction, which proceeds through a putative diimide intermediate, displays high tolerance to a variety of functional groups, including those sensitive to nucleophilic displacement by hydrazine, aerobic oxidation, or hydrazine-mediated reduction. Hydrazine chemisorbs strongly to the carbon surface, attenuating its native oxidative reactivity and allowing for selective hydrogenation. The catalytic sequence established here effectively umpolungs the reactivity of carbon, thereby enabling the use of this low cost material in selective reduction catalysis.

Introduction

Heterogeneous hydrogenation catalysts mediate critical transformations in the synthesis of value-added fine and commodity chemicals as well as pharmaceuticals.[1] With rare exception, these catalysts consist of active transition metal-based extended solids or molecular fragments that carry out the hydrogenation using molecular hydrogen or a hydrogen carrier as the terminal reductant. Despite many decades of optimization, metal-based heterogeneous hydrogenation catalysts still suffer from two key limitations: they often require platinum group metals which may pose cost and resource limitations, particularly for large scale commodity manufacturing, and the immobilized metal atoms may leach into the reactant stream, which, even at trace levels, compromises product purity for pharmaceutical applications.[2–4] Despite significant development of homogeneous metal-free hydrogenation reactions, there exist a relative paucity of analogous metal-free heterogeneous reactions. The few examples that do exist are postulated to proceed *via* frustrated Lewis pair type mechanisms,[5] including one utilizing graphene oxide as a catalyst.[6] Frustrated Lewis pair methodologies are also applicable to dehydrogenation[7] and CO_2 reduction chemistries.[8] Additionally, recent examples exist for graphene or doped graphene-mediated hydrogenation reactions using high-pressure H_2.[9,10] Nevertheless, the development of new robust metal-free heterogeneous catalytic processes for olefin hydrogenation is needed to overcome the above limitations and enable more sustainable chemical processing.

Recent studies have established graphitic carbon materials as potent aerobic oxidation catalysts for a variety of organic substrates.[11–20] These oxidations are postulated to be mediated by quinoid and other oxidic functional groups that are known to populate the edge-plane surface terminations of nearly all graphitic carbon materials.[21–23] Given the relatively high redox potential of most quinone/catechol couples, these sites are unable to mediate reduction catalysis except for the most oxidizing of substrates (e.g. nitroaromatics).[24–26] To circumvent this inherent limitation, we sought to combine graphitic carbon with a terminal reductant that could be activated via aerobic two electron oxidation, thereby inverting the native reactivity of graphitic carbon and enabling metal-free heterogeneous hydrogenation catalysis.

Hydrazine hydrate is a readily available hydrogen carrier and reductant that is commonly applied in the metal-catalyzed reduction of nitroarenes[27,28] and it is known that two-electron, two-proton oxidation of hydrazine generates diimide, N_2H_2, a far more potent hydrogenating agent, that is known to rapidly reduce primary and secondary olefins.[29] In addition to transition metals such as Cu(II),[30,31] flavin derivatives,[32–35] and quinones[36] are known to generate diimide via two-electron, two-proton oxidation of hydrazine (Figure 1). Given the large population of quinoid moieties on graphitic carbon surfaces, we postulated that extremely low-cost carbon blacks would be able to catalyze aerobic hydrazine oxidation to diimide which could transfer an H_2 equivalent to olefin substrate with liberation of N_2. Herein, we show that commercially available carbon blacks effectively catalyze the selective reduction of olefins to alkanes with hydrazine as the terminal reductant.

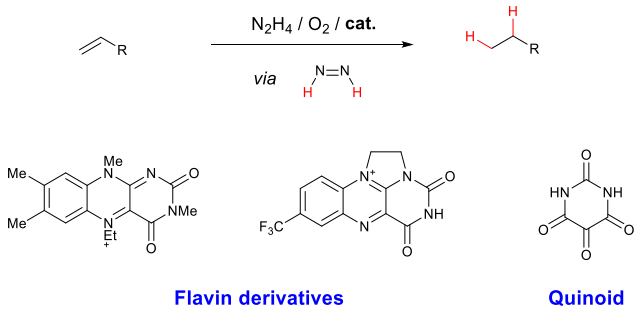

Figure. 1. General depiction of diimide reduction and examples of previous catalysts

Results and Discussion

Using octadecene **1a** as a test substrate, we evaluated a variety of commercially available carbon blacks for olefin hydrogenation under aerobic conditions with hydrazine as the terminal reductant. We found that all high surface area carbons examined gave significantly increased reactivity relative to the un-catalyzed background. In particularly, the rate of conversion after 20 minutes loosely correlate to their surface areas as determined by gas sorption analysis applying a BET isotherm (Figure 2) with mesoporous carbon being an outlier due to lower oxygen content (see below). The highest surface area carbon explored, Cabot Monarch 1300 carbon black, proved to be the optimal carbocatalyst for this transformation. Using this carbon, we observed continued conversion with longer reaction times, reaching 50% conversion to the hydrogenated product after 60 minutes at 40 °C (Table S1). Interestingly, we observed a slow background reaction in the absence of carbon which we attribute to sluggish direct oxidation of hydrazine by O_2 (Table S1). The reaction displays no appreciable solvent dependence with non-polar solvents such as toluene displaying similar conversion to more polar acetonitrile and methanol (Table S2). Ultimately, THF was chosen for subsequent studies due to its combination of miscibility with hydrazine hydrate and its ability to disperse the carbon effectively.[37]

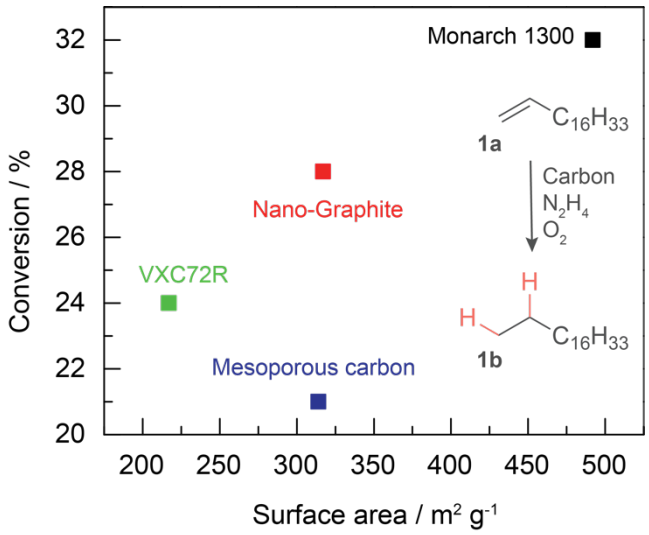

Figure 2. Percent conversion at the 20 min time point vs carbon surface area for hydrogenation of octadecene by hydrazine under aerobic conditions.

ICP-MS analysis of the most active carbon suggests that trace metal ion impurities play a minimal role in the catalysis. Cu^{2+} is known to catalyze aerobic oxidation of hydrazine to diimide, and Pd metal is a potent hydrogenation catalyst. ICP-MS analysis of acid digested Monarch 1300 samples reveals trace metal fractions of 0.5 µg Cu and 0.2 µg Pd per gram of carbon black. Based on the catalyst loadings used in this study, these values correspond to 50 ng and 20 ng of Cu and Pd in the reaction mixture. These values are far below the lowest reported metal loadings of ~100 µg of Cu for this reaction.[38] Additionally, if these trace metals were to leach quantitatively from the carbon during the reaction, the highest metal concentrations expected during any of the reactions examined here are 263 fM and 63 fM for Cu and Pd, respectively, which are far lower than the Cu concentrations of ~1 mM utilized in homogeneous hydrazine-based hydrogenations.[30] All of the other carbon samples also have undetectable amounts of Pd and Mn, and low ppb levels of Fe and Cu in all cases (Table S3). Together, the data suggest that the observed reactivity is unlikely to be due to trace levels of transition metals but is rather due to the intrinsic catalytic reactivity of the carbon surface.

The mechanism by which carbon catalyzes oxidation of hydrazine remains largely unknown. It has been postulated that hydrogen bonding between hydrazine and oxidic functional groups on carbon can active this molecule toward oxidation.[39] This postulate implies that hydrazine and carbon do not engage in extensive covalent bond formation.[40] Conversely, a systematic study of the addition of hydrazine to graphene oxide revealed the formation of surface pyrazoline and pyrazole moieties.[41] To gain further insight into the nature of the surface during catalysis, we examined the Monarch 1300 carbon by IR and X-ray photoelectron spectroscopy following hydrazine treatment. Difference IR spectra reveal a pronounced bleach at 1640 – 1800 cm^{-1} upon hydrazine treatment suggesting condensation or reduction of surface oxidic functional groups such as quinones, ketones and/or carboxylic acids (Figure 3, left). XPS spectra of hydrazine-treated Monarch 1300 contain a pronounced broad nitrogen 1s peak (Figure 3, right) centered at 401 eV. Owing to the breadth of this peak (FWHM = 3.0 eV), which spans characteristic peak positions expected for amine and imine moieties,[42] we are unable to assign a single dominant nitrogen environment on the surface. Notably, the absence of a second peak at <400 eV suggests the surface does not consist of a majority of pyridinic or pyrazolic nitrogen moieties.[41] This rise in surface N fraction from ~0% to 1.7% is accompanied by a large decrease in surface O fraction from 7.1% to 4.5% (Table S5), and a reduction of XPS O 1s signal intensity at binding energies >533 eV, attributed to reduction in surface C=O groups (Figure S3). This suggests a significant fraction of the surface oxidic functional groups undergo condensation with hydrazine under the reaction conditions. The carbon 1s peak remains predominantly graphitic, indicating that exposure to hydrazine has not dramatically altered the bulk carbon (Figure S4). The radical alteration of the surface chemistry of carbon upon reaction with hydrazine is expected to attenuate its native oxidation reactivity which we postulate is essential for the selective catalysis described below.

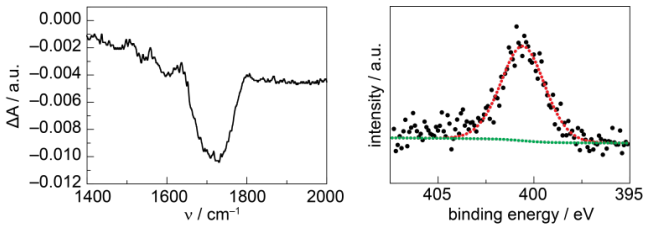

Figure 3. (Left) Difference FTIR spectra of hydrazine-treated Monarch 1300 carbon black relative to native Monarch 1300 carbon black. (Right) High resolution XPS N 1s spectrum of Monarch 1300 carbon (Data = black, Fit = red, Background = green).

As the aerobic oxidation of hydrazine has been shown to occur on quinone-containing molecular catalysts,[32,36] we sought to probe the role of these surface functional groups on catalysis mediated by the carbon surface. We treated Monarch 1300 samples with either 2,4-dinitrophenylhydrazine or 1,2-phenylenediamine (Figure S6), which are known to undergo site-selective condensation reactions with surface ketone and o-quinone moieties, respectively.[22,23] In both cases, the modi-

fied surfaces display only marginally decreased rates of catalysis suggesting that surface ketone and quinone moieties are not uniquely responsible for catalysis. We also observe no correlation between catalytic activity and the population of surface *o*-quinone moieties (Table S6).[23,43] Nonetheless, we observe a correlation between activity and the total oxygen context of the carbon and this partly explains the low activity of mesoporous carbon despite its high surface area (Figure 2). However, carbon samples with minimal oxygen content still promote catalysis (Figure S7), suggesting that oxidic functional groups may play a promoting role, but are not uniquely necessary for catalysis. Indeed, it is possible that protonated oxidic functional groups may enhance the rate of catalysis by facilitating proton coupled surface reactions involving O_2 activation or hydrazine oxidation.[15,37] Combined, these observations lead us to propose that the carbon surface effects aerobic oxidation of hydrazine via a superoxide intermediate bound non-specifically to sites of high spin density on the carbon surface, which are known to exist even in the absence of significant surface oxidation. [15,44,45]

Reaction time course data provide qualitative insight into the mechanism of this reaction. Importantly, we observe negligible conversion (~2%) when the reaction is conducted in the absence of O_2 (Figure 4 blue triangle) indicating that the reaction requires two-electron oxidation of hydrazine to generate the putative diimide intermediate. This observation also indicates that the reaction does not proceed via a transfer hydrogenation-mechanism with surface bound H as an intermediate.

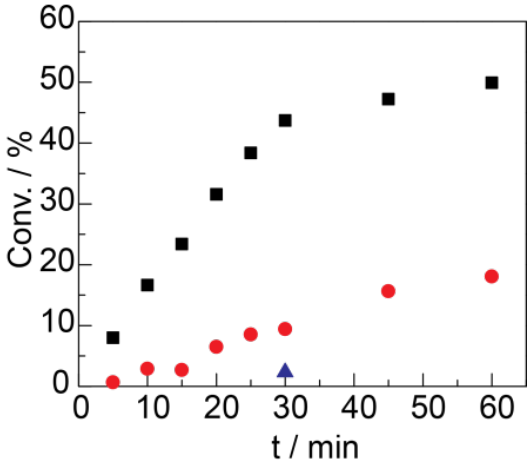

Figure 4. Reduction of octadecene **1a** vs. time normalized vs. an internal standard of naphthalene, in presence of Monarch 1300 carbon (black), no catalyst (red), and a single point under N_2 atmosphere (blue) as measured by GC.

In the presence of O_2, we observe relatively rapid initial reaction progress, leading to ~50% conversion to product after 30 minutes (Figure 4, black squares) that far outpaces the rate of the uncatalyzed reaction (Figure 4, red circles). This rapid product formation is followed by an effective plateau in reaction progress at longer times. This abrupt attenuation in reaction rate after ~30 min is attributed to nearly complete consumption of the terminal N_2H_4 reductant over this time period. Notably, the reaction stalls despite the presence of 2.5 eq of N_2H_4 relative to the alkene. These observations are consistent with the following mechanistic sequence (Scheme 1):

Scheme 1. Proposed mechanistic sequence for Monarch 1300 carbon catalyzed olefin hydrogenation.

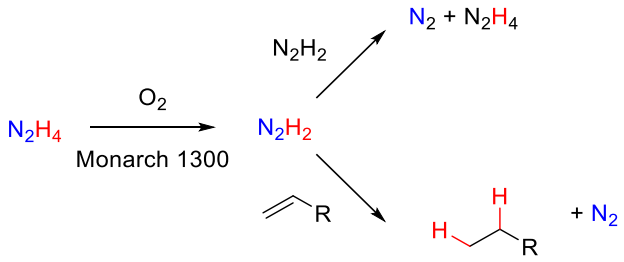

This sequence invokes carbocatalyzed aerobic oxidation of N_2H_4 to N_2H_2, which can than undergo disproportionation to generate N_2H_4 and N_2 or reaction with the olefin to generate the hydrogenated product. As the disproportionation reaction is bimolecular in N_2H_2 and the hydrogenation is unimolecular in N_2H_2, the former is strongly favored under conditions in which N_2H_2 is generated rapidly. Thus, simply increasing the N_2H_4 concentration is counterproductive because it serves to accelerate the disproportionation route preferentially over the hydrogenation. Instead, the pool of N_2H_2 must be kept relatively low over the course of the reaction, but sufficient N_2H_2 must be present to effect rapid hydrogenation.

Indeed, we find that product conversion can be maximized via sequential additions of N_2H_4 and we found that this protocol is very effective for the hydrogenation a wide variety of olefins (Scheme 2 and Table S7). We generally performed the reaction at 40 °C under one atmosphere of oxygen with sequential addition of 2.5 equivalents of hydrazine at the 0, 1, and 2 hour time points. The reaction was then allowed to proceed for another 22 hours before workup, giving a quantitative yield of **1b** (Scheme 2, upper right). Additionally, we find that controlled N_2H_4 addition using a syringe pump gives rise to good hydrogenation activity (Supporting Information, page S5) with a four-fold lower mass loading of the carbon. Owing to the combination of a heterogeneous catalyst and a gaseous byproduct, N_2, the product could be isolated simply via brief centrifugation of the reaction mixture at 7000 rpm followed by removal of the solvent from the supernatant under vacuum. The operational simplicity of this workup procedure relative to the more laborious separations required for homogeneously catalyzed reactions may make this method particularly attractive for process and flow chemistries. Additionally, the reaction can be run at ambient temperature in the presence of air rather than 1 atm of O_2 (Table S7). This further reduces the process demands and potential hazards for large scale hydrogenations.[46]

Scheme 2. Monarch 1300 carbon-catalyzed hydrogenation of selected substrates compared to alternative reactive conditions.

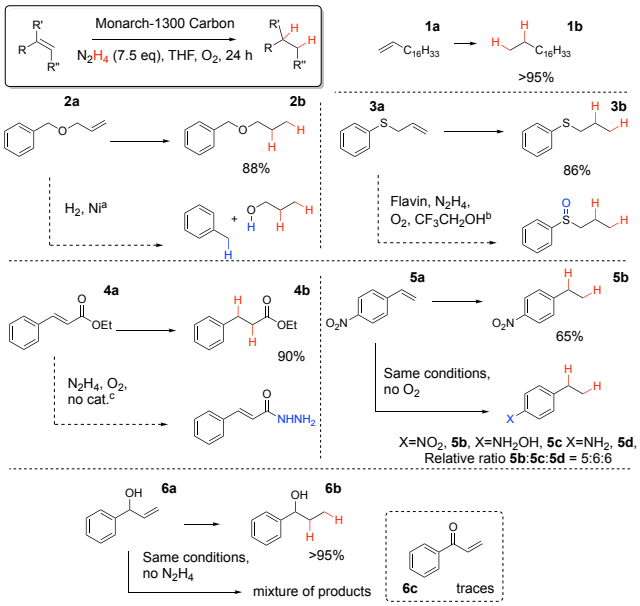

[a]Ref. 49 [b]Ref. 32 [c]Ref. 50

The heterogeneous hydrogenation sequence developed here offers some distinct advantages relative to heterogeneous transition-metal based hydrogenations. For example, selective olefin hydrogenation relative to hydrogenolysis in substrates such as **2a**, is particularly challenging at heterogeneous metal surfaces, requiring specialty supports[47,48] and/or careful reaction monitoring even for relatively low activity nickel-based hydrogenation catalysts.[49] In line with the high selectivity of diimide for relatively non-polar double bonds over other reducible functional groups, the sequence developed here selectivity reduces the olefin to generate **2b** without cleavage of the sensitive benzyl ether. Additionally, metal surfaces are known to strongly adsorb sulfur-containing molecules, and thus sulfides such as **3a** are expected to be poisoned by traditional metal-based heterogeneous catalysts and we are unaware of any such catalyst that mediates the hydrogenation of this substrate. Under our reaction conditions, the allyl sulfide **3a** is smoothly hydrogenated to **3b** in high yield. Together, these two examples serve to highlight the potential advantages of this catalytic sequence relative to traditional metal-based heterogeneous hydrogenations.

As hydrazine is a potent nucleophile, it has been found to be incompatible with carbonyl groups.[50] Indeed, substrates such as cinnamate **4a** undergo ester cleavage and hydrazide formation rather than hydrogenation under similar aerobic conditions in the absence of catalyst. In contrast, under carbon-catalyzed reaction conditions, we observe selective formation of the hydrogenated product, **4b**, in good yield. Thus, carbon-catalyzed aerobic oxidation of hydrazine serves to keep the pool of this nucleophile low, thereby impeding the displacement reaction relative to hydrogenation via the diimide intermediate.

The reaction conditions employed here permit selective hydrogenation without interfering reduction of other sensitive functional groups. For 4-nitrostyrene **5a,** we observe exclusive reduction of the olefin over the nitro group, yielding saturated nitroarene **5b.** Although selective alkene reduction in the presence of nitro groups is well documented for hydrazine mediated reductions with Cu catalysts,[38] the thermodynamic driving force for reducing a nitro group,[51] ΔH_{red} = 85 kcal mol^{-1}, is significantly greater than that for reducing an alkene,[52] ΔH_{red} = –33 kcal mol^{-1}, making the former a more facile reaction in general.[53] Notably, graphitic carbons can catalyze the *anaerobic* reduction of nitroarenes to anilines with N_2H_4.[24] Diimide is not thought to be the active intermediate in these reactions.[25] Upon repeating the reaction in the absence of O_2, we observed a mixture of **5b**, hydroxylamine **5c,** and aniline **5d** (Figure 3).[54] These observations suggest that the aerobic conditions are essential for preventing carbon-catalyzed nitro group reduction by hydrazine. Although the diimide intermediate is known to be selective for olefin hydrogenation over nitro reduction, our observations also indicate that carbon-catalyzed aerobic oxidation of hydrazine outcompetes hydrazine mediated reduction of nitroarenes under these reaction conditions, enabling high reaction selectivity.

In addition to enabling hydrogenation reactivity mediated by diimide, the presence of hydrazine serves to attenuate the inherent oxidative reactivity of carbon. For example, the hydrogenation of alcohol **6a** proceeded quantitatively to **6b** in the presence of hydrazine, with complete preservation of the oxidatively sensitive allyl benzyl alcohol moiety. In the absence of hydrazine, this reaction generates an ill-defined mixture of decomposition products (32 observable ^{13}C NMR peaks). Indeed, minor amounts of both enone[55] **6c** and an unknown aldehyde are observed in the ^{1}H NMR spectrum suggestive of carbon-mediated aerobic oxidation reactivity.[56]

Likewise, we do not observe any oxidation of sulfide **3a** to the corresponding sulfoxide in the presence of hydrazine. This is noteworthy given that under similar reaction conditions, flavin organocatalysts can mediate sulfoxide formation from the same substrate via a putative bound-peroxo intermediate.[32] Together, these observations highlight that hydrazine serves to umpolung the native oxidative reactivity of carbon. Given the large population of chemisorbed nitrogen species on the surface, we postulate that hydrazine's strong interaction with the surface is critical for enabling selective hydrogenation reactivity.

Despite the pronounced alteration of the surface chemistry of carbon in the presence of hydrazine, the carbon catalyst is nonetheless somewhat recyclable. Using 1-octadecene, **1a**, as the test substrate, isolation and reintroduction of the catalyst to subsequent batch runs led to similar levels of conversion over three cycles of reuse with a modest reduction in reactivity thereafter (Figure S8). To probe the origin of this modest deactivation we examine carbon samples after 4 catalytic runs by TGA and XPS.

Thermogravimetric analysis (TGA) of Monarch 1300 samples prior to and following hydrazine treatment reveals similar mass loss profiles apart from the expected low temperature (100 to 150 C) mass loss attributed to adsorbed hydrazine and solvent. However, TGA of Monarch 1300 following catalyst deactivation, reveals a pronounced 25% mass loss over the 200-270 °C range, in line with the formation of a passivating oligomeric or polymeric film on the surface of the carbon (Figure S9).

XPS analysis is also consistent with the formation of passivating film on the carbon surface. The properties of the carbon catalyst after one cycle of catalysis are essentially identical to carbon treated with hydrazine alone in the absence of substrate. However, after four cycles of catalysis, non-graphitic impurities are visible in the C 1s high-resolution XPS spectrum (Figure S11) and this is accompanied by a rise

in the intensity of the oxygen and nitrogen 1s XPS signals as well. These observations suggest that the surface is covered with an adsorbed passivating film, which may arise from adventitious adsorption and polymerization of the THF solvent.[57]

Conclusions

We have developed an operationally simple, metal-free heterogeneous catalytic system for selective hydrogenation of carbon-carbon double bonds. The reaction is highly tolerant of sensitive functional groups and proceeds *via* a putative diimide intermediate generated by carbon-catalyzed aerobic oxidation of hydrazine. The hydrazine chemisorbs strongly to the carbon surface and serves to attenuate its oxidative reactivity, allowing for selective substrate hydrogenation under aerobic conditions. Thus, this catalytic sequence serves to reverse the native aerobic oxidation reactivity of carbon, opening the door for the use of this low cost material to catalyze a wider variety of substrate transformations.

ASSOCIATED CONTENT

Full experimental details, expanded substrate scope, additional XPS, IR, ICP-MS and TGA data, ^{1}H and ^{13}C NMR spectra for all products. This material is available free of charge via the Internet at http://pubs.acs.org.

AUTHOR INFORMATION

Corresponding Author

*yogi@mit.edu

ACKNOWLEDGMENT

We thank Yuri Roman-Leshkov for access to gas chromatography, Mircea Dincă for access to gas adsorption analysis, and thank Adam Rieth for assistance with gas adsorption. This research was funded by the U.S. Department of Energy, Office of Science, Office of Basic Energy Sciences, under award number DE-SC0014176 and by the MIT Department of Chemistry through junior faculty funds for Y.S. Additionally, A.T.M. was supported by a Dreyfus Postdoctoral Fellowship.

REFERENCES

(1) Shigeo Nishimura. *Handbook of Heterogeneous Catalytic Hydrogenation for Organic Synthesis*; WILEY- VCH Verlag, 2001.
(2) Friedman, D.; Masciangioli, T.; Olson, S. *The role of the chemical sciences in finding alternatives to critical resources*; 2011.
(3) Teasdale, A. *Org. Process Res. Dev.* **2015**, *19*, 1725–1730.
(4) Miyamoto, H.; Sakumoto, C.; Takekoshi, E.; Maeda, Y.; Hiramoto, N.; Itoh, T.; Kato, Y. *Org. Process Res. Dev.* **2015**, *19*, 1054–1061.
(5) Nash, D. J.; Restrepo, D. T.; Parra, N. S.; Giesler, K. E.; Penabade, R. A.; Aminpour, M.; Le, D.; Li, Z.; Farha, O. K.; Harper, J. K.; Rahman, T. S.; Blair, R. G. *ACS Omega* **2016**, *1*, 1343–1354.
(6) Primo, A.; Neatu, F.; Florea, M.; Parvulescu, V.; Garcia, H. *Nat. Commun.* **2014**, *5*, 5291.
(7) Grant, J. T.; Carrero, C. A.; Goeltl, F.; Venegas, J.; Mueller, P.; Burt, S. P.; Specht, S. E.; McDermott, W. P.; Chieregato, A.; Hermans, I. *Science* **2016**, *354*, 1570–1573.
(8) Ghuman, K. K.; Hoch, L. B.; Szymanski, P.; Loh, J. Y. Y.; Kherani, N. P.; El-Sayed, M. A.; Ozin, G. A.; Singh, C. V. *J. Am. Chem. Soc.* **2016**, *138*, 1206–1214.
(9) Trandafir, M. M.; Florea, M.; Neațu, F.; Primo, A.; Parvulescu, V. I.; Garcia, H. *ChemSusChem* **2016**, *9*, 1565–1569.
(10) Liu, R.; Li, F.; Chen, C.; Song, Q.; Zhao, N.; Xiao, F. *Catal. Sci. Technol.* **2017**, *7*, 1217–1226.
(11) Navalon, S.; Dhakshinamoorthy, A.; Alvaro, M.; Garcia, H. *Chem. Rev.* **2014**, *114*, 6179–6212.
(12) Peng, W.; Liu, S.; Sun, H.; Yao, Y.; Zhi, L.; Wang, S. *J. Mater. Chem. A* **2013**, *1*, 5854.
(13) Cao, Y.; Luo, X.; Yu, H.; Peng, F.; Wang, H.; Ning, G. *Catal. Sci. Technol.* **2013**, *3*, 2654.
(14) Sun, H.; Liu, S.; Zhou, G.; Ang, H. M.; Tadé, M. O.; Wang, S. *ACS Appl. Mater. Interfaces* **2012**, *4*, 5466–5471.
(15) Su, C.; Acik, M.; Takai, K.; Lu, J.; Hao, S.; Zheng, Y.; Wu, P.; Bao, Q.; Enoki, T.; Chabal, Y. J.; Ping Loh, K. *Nat. Commun.* **2012**, *3*, 1298.
(16) Li, W.; Gao, Y.; Chen, W.; Tang, P.; Li, W.; Shi, Z.; Su, D.; Wang, J.; Ma, D. *ACS Catal.* **2014**, *4*, 1261–1266.
(17) Yang, J.-H.; Sun, G.; Gao, Y.; Zhao, H.; Tang, P.; Tan, J.; Lu, A.-H.; Ma, D. *Energy Environ. Sci.* **2013**, *6*, 793.
(18) Gao, Y.; Hu, G.; Zhong, J.; Shi, Z.; Zhu, Y.; Su, D. S.; Wang, J.; Bao, X.; Ma, D. *Angew. Chem. Int. Ed.* **2013**, *52*, 2109–2113.
(19) Gao, Y.; Tang, P.; Zhou, H.; Zhang, W.; Yang, H.; Yan, N.; Hu, G.; Mei, D.; Wang, J.; Ma, D. *Angew. Chem. Int. Ed.* **2016**, *55*, 3234–3234.
(20) Tang, P.; Hu, G.; Li, M.; Ma, D. *ACS Catal.* **2016**, *6*, 6948–6958.
(21) Boehm, H.-P.; Diehl, E.; Heck, W.; Sappok, R. *Angew. Chem. Int. Ed. English* **1964**, *3*, 669–677.
(22) Thorogood, C. A.; Wildgoose, G. G.; Jones, J. H.; Compton, R. G. *New J. Chem.* **2007**, *31*, 958–965.
(23) Fukushima, T.; Drisdell, W.; Yano, J.; Surendranath, Y. *J. Am. Chem. Soc.* **2015**, *137*, 10926–10929.
(24) Hee Ha, B.; Hyun Shin, D.; Yun Cho, S. *Tetrahedron Lett.* **1985**, *26*, 6233–6234.
(25) Larsen, J. W.; Freund, M.; Kim, K. Y.; Sidovar, M.; Stuart, J. L. *Carbon* **2000**, *38*, 655–661.
(26) Gao, Y.; Ma, D.; Wang, C.; Guan, J.; Bao, X. *Chem. Commun.* **2011**, *47*, 2432–2434.
(27) Shi, Q.; Lu, R.; Lu, L.; Fu, X.; Zhao, D. *Adv. Synth. Catal.* **2007**, *349*, 1877–1881.
(28) Li, F.; Frett, B.; Li, H. Y. *Synlett* **2014**, *25*, 1403–1408.
(29) Pasto, D. J.; Taylor, R. T.; Pasto, D. J.; Taylor, R. T. In *Organic Reactions*; John Wiley & Sons, Inc.: Hoboken, NJ, USA, 1991; pp 91–155.
(30) Corey, E. J.; Mock, W. L.; Pasto, D. J. *Tetrahedron Lett.* **1961**, *2*, 347–352.
(31) Corey, E. J.; Pasto, D. J.; Mock, W. L. *J. Am. Chem. Soc.* **1961**, *83*, 2957–2958.
(32) Imada, Y.; Iida, H.; Naota, T. *J. Am. Chem. Soc.* **2005**, *127*, 14544–14545.
(33) Smit, C.; Fraaije, M. W.; Minnaard, A. J. *J. Org. Chem.* **2008**, *73*, 9482–9485.
(34) Imada, Y.; Kitagawa, T.; Ohno, T.; Iida, H.; Naota, T. *Org. Lett.* **2010**, *12*, 32–35.
(35) Marsh, B. J.; Heath, E. L.; Carbery, D. R. *Chem. Commun.* **2011**, *47*, 280–282.
(36) Murray, A. T.; King, R.; Donnelly, J. V. G.; Dowley, M. J. H.; Tuna, F.; Sells, D.; John, M. P.; Carbery, D. R. *ChemCatChem* **2016**, *8*, 510–514.
(37) Chu, S. B.; Fukushima, T.; Surendranath, Y. *Chem. Mater.* **2017**, *29*, 495–498.
(38) Dhakshinamoorthy, A.; Navalon, S.; Sempere, D.; Alvaro, M.; Garcia, H. *Chem. Commun* **2013**, *49*, 2359–2361.
(39) Wu, S.; Wen, G.; Liu, X.; Zhong, B.; Su, D. S. *ChemCatChem* **2014**, *6*, 1558–1561.
(40) Wu, S.; Wen, G.; Wang, J.; Rong, J.; Zong, B.; Schlögl, R.; Su, D. S. *Catal. Sci. Technol* **2014**, *4*, 4183–4187.
(41) Park, S.; Hu, Y.; Hwang, J. O.; Lee, E.-S.; Casabianca, L. B.; Cai, W.; Potts, J. R.; Ha, H.-W.; Chen, S.; Oh, J.; Kim, S. O.; Kim, Y.-H.; Ishii, Y.; Ruoff, R. S. *Nat. Commun.* **2012**, *3*, 638.
(42) Golczak, S.; Kanciurzewska, A.; Fahlman, M.; Langer, K.; Langer, J. J. *Solid State Ion.* **2008**, *179*, 2234–2239.
(43) Oh, S.; Gallagher, J. R.; Miller, J. T.; Surendranath, Y. *J. Am. Chem. Soc.* **2016**, *138*, 1820–1823.
(44) Appleby, A. J.; Marie, J. *Electrochim. Acta* **1979**, *24*, 195–202.
(45) Yeager, E. *J. Mol. Catal.* **1986**, *38*, 5–25.
(46) Osterberg, P. M.; Niemeier, J. K.; Welch, C. J.; Hawkins, J. M.; Martinelli, J. R.; Johnson, T. E.; Root, T. W.; Stahl, S. S. *Org. Process Res. Dev.* **2015**, *19*, 1537–1543.
(47) Banerjee, S.; Balasanthiran, V.; Koodali, R. T.; Sereda, G. A.

Org. Biomol. Chem. **2010**, *8*, 4316.
(48) Monguchi, Y.; Marumoto, T.; Ichikawa, T.; Miyake, Y.; Nagae, Y.; Yoshida, M.; Oumi, Y.; Sawama, Y.; Sajiki, H. *ChemCatChem* **2015**, *7*, 2155–2160.
(49) Perosa, A.; Tundo, P.; Zinovyev, S. *Green Chem.* **2002**, *4*, 492–494.
(50) Pieber, B.; Martinez, S. T.; Cantillo, D.; Kappe, C. O. *Angew. Chem. Int. Ed.* **2013**, *52*, 10241–10244.
(51) Roberts, J. D.; Caserio, M. C. *Basic Principles of Organic Chemistry*, 2nd ed.; Caltech University Press: Menlo Park, CA, 1977.
(52) Cottrell, T. L. *The Strength of Chemical Bonds*, 2nd ed.; Butterworth and co.: London, 1958.
(53) Blaser, H. U.; Steiner, H.; Studer, M. *ChemCatChem* **2009**, *1*, 210–221.
(54) Marques, M. M.; Mourato, L. L. G.; Amorim, M. T.; Santos, M. A.; Melchior, W. B.; Beland, F. A. *Chem. Res. Toxicol.* **1997**, *10*, 1266–1274.
(55) Shen, D.; Miao, C.; Xu, D.; Xia, C.; Sun, W. *Org. Lett.* **2015**, *17*, 54–57.
(56) Dreyer, D. R.; Jia, H. P.; Bielawski, C. W. *Angew. Chem. Int. Ed.* **2010**, *49*, 6813–6816.
(57) Heins, C. F. *J. Polym. Sci. Part B Polym. Lett.* **1969**, *7*, 625–626.

Insert Table of Contents artwork here